Cotreatment with BCL-2 antagonist sensitizes cutaneous T-cell lymphoma to lethal action of HDAC7-Nur77–based mechanism

Jianguang Chen,[1] Warren Fiskus,[1] Kelly Eaton,[1] Pravina Fernandez,[1] Yongchao Wang,[1] Rekha Rao,[1] Pearl Lee,[1] Rajeshree Joshi,[1] Yonghua Yang,[1] Ravindra Kolhe,[1] Ramesh Balusu,[1] Prasanthi Chappa,[1] Kavita Natarajan,[1] Anand Jillella,[1] Peter Atadja,[2] and Kapil N. Bhalla[1]

[1]Medical College of Georgia Cancer Center, Augusta; and [2]Novartis Institute for Biomedical Research, Cambridge, MA

Pan-histone deacetylase inhibitors, for example, vorinostat and panobinostat (LBH589; Novartis Pharmaceuticals, East Hanover, NJ), have shown clinical efficacy against advanced cutaneous T-cell lymphoma (CTCL). However, the molecular basis of this activity remains unclear. HDAC7, a class IIA histone deacetylase (HDAC), is overexpressed in thymocytes, where it represses expression of the proapoptotic nuclear orphan receptor Nur77. Here, we demonstrate that treatment with panobinostat rapidly inhibits the in vitro and intracellular activity, as well as the mRNA and protein levels of HDAC7, and induces expression and translocation of Nur77 to the mitochondria. There, Nur77 converts death resistance protein Bcl-2 into a killer protein, promoting cell death of cultured and patient-derived human CTCL cells. Treatment with panobinostat improved survival of athymic nude mice implanted with human CTCL cells. Ectopic expression of Nur77 induced apoptosis and sensitized HH cells to panobinostat, whereas combined knockdown of Nur77 and its family member Nor1 was necessary to inhibit panobinostat-induced apoptosis of CTCL cells. Cotreatment with the Bcl-2/Bcl-x_L antagonist ABT-737 decreased resistance and synergistically induced apoptosis of human CTCL cells. These findings mechanistically implicate HDAC7 and Nur77 in sensitizing human CTCL cells to panobinostat as well as suggest that cotreatment with an anti–Bcl-2 agent would augment the anti-CTCL activity of panobinostat. (Blood. 2009; 113:4038-4048)

Introduction

Cutaneous T-cell lymphoma (CTCL) is a relatively uncommon, indolent variety of non-Hodgkin lymphoma with involvement of the skin by neoplastic $CD4^+$ T lymphocytes.[1-3] Pan-histone deacetylase (HDAC) inhibitors (HDIs), including depsipeptide, vorinostat, and panobinostat, have demonstrated clinical efficacy in CTCL, and vorinostat is currently approved and available as treatment for CTCL.[4-6] Compared with vorinostat, depsipeptide is a significantly more potent and relatively selective inhibitor of class I HDACs.[7] Although objective clinical responses are observed in approximately 30% of patients, treatment with vorinostat eventually fails, indicating the need to develop new and more effective therapies for CTCL.[8,9] Both vorinostat and panobinostat (LBH589) are hydroxamic acid analog HDIs, which inhibit class I, IIA, and IIB histone deacetylases and induce acetylation of histones and nonhistone proteins.[7,10] The biologic activity of class II HDACs, including HDAC7, is also determined by their subcellular localization, because they shuttle between the cytoplasm and nucleus.[11] Recently, vorinostat was shown to down-regulate the expression of HDAC7 in several cancer cell lines.[12] HDAC7 is highly expressed in double-positive ($CD4^+$ $CD8^+$) T lymphocytes, where it regulates antigen-induced apoptosis and negative selection of thymocytes.[13] In the nucleus of resting thymocytes, HDAC7 interacts with the transcriptional regulator MEF2D, which binds to the promoters and transcriptionally represses the proapoptotic nuclear orphan receptor NR4A family members Nur77 (NR4A1) and Nor1.[13,14] After T-cell receptor (TCR) activation, phosphorylation and export of HDAC7 from the nucleus into the cytoplasm and mitochondria results in derepression of Nur77 and Nor1.[14,15] Conversely, dephosphorylation of HDAC7 promotes nuclear localization of HDAC7, causing repression of Nur77 and inhibition of apoptosis of $CD4^+$ $CD8^+$ thymocytes.[15,16]

As orphan nuclear receptors, Nur77 and Nor1 have no known physiologic ligands, but through their interaction with retinoid X receptor (RXR) and transcriptional activity promote growth and survival of cancer cells.[17,18] Previously, high levels of Nor1 expression have been correlated with favorable responses to chemotherapy in diffuse large B-cell lymphoma.[19] Nur77 has also been shown to lower the threshold for apoptosis by transcriptionally altering the levels of apoptosis regulatory proteins.[20] Ectopic overexpression of Nur77 in thymocytes induces massive apoptosis.[21] After an apoptotic stimulus, Nur77 was shown to translocate to the mitochondria and bind to the N-terminal loop region between the BH4 and BH3 domain of Bcl-2, Bcl-x_L, or Bcl-B.[22-24] This conformationally converts Bcl-2 from an antiapoptosis to a prodeath killer protein, triggering mitochondrial cytochrome *c* release, caspase activation, and apoptosis.[24,25] Because Nur77 is functionally redundant with Nor1, Nur77-null mice do not have a phenotype.[21] However, a dominant negative Nur77 protein that blocks the activity of both Nur77 and Nor1 also attenuated apoptosis during negative selection,[26,27] and Nur77 transgenic mice exhibit massive apoptosis of thymocytes.[28] Recently, abrogation of Nur77 and Nor1 in mice was shown to induce rapidly lethal acute leukemia.[29] In the present studies, we show that panobinostat treatment significantly delays tumor growth and increases survival of human CTCL

Submitted August 27, 2008; accepted November 28, 2008. Prepublished online as *Blood* First Edition paper, December 12, 2008; DOI 10.1182/blood-2008-08-176024.

The online version of this article contains a data supplement.

The publication costs of this article were defrayed in part by page charge payment. Therefore, and solely to indicate this fact, this article is hereby marked "advertisement" in accordance with 18 USC section 1734.

xenograft in nude mice. In cultured and primary CTCL cells, treatment with the pan-HDAC inhibitor panobinostat depletes HDAC7 expression and activity, thereby simultaneously inducing Nur77 and Nor1. After its induction, Nur77 translocates to the mitochondria and triggers apoptosis. In addition, our findings show that combined treatment of panobinostat and ABT-737, which is a small molecule inhibitor of the antiapoptotic Bcl-2, Bcl-x_L, and Bcl-B proteins,[30,31] induces synergistic apoptosis of both the HDAC inhibitor–sensitive as well as the HDAC inhibitor–insensitive cells.

Methods

Reagents, plasmids, and antibodies

Panobinostat was kindly provided by Novartis Pharmaceuticals (East Hanover, NJ). ABT-737 was provided by Abbott Laboratories (Abbott Park, IL). Anti-HDAC7, anti-Nur77, anti-pSTAT3 (Tyr705), anti-pSTAT1 (Tyr701), and anti-STAT1 were obtained from Cell Signaling (Beverly, MA). Antitubulin and antiacetylated tubulin antibodies were obtained from Sigma-Aldrich (St Louis, MO). Anti-STAT5 and anti-STAT3 were obtained from Santa Cruz Biotechnology (Santa Cruz, CA). Antibody for detection of Nur77 (ab48789) by confocal microscopy was purchased from Abcam (Cambridge, MA). Antibodies for the immunoblot analysis of PARP, caspase-3, Bax, Bak, Bcl-2, Bim, XIAP, MCL-1, BAD, Bcl-x_L, pSTAT5 (Tyr694), and β-actin were obtained as previously described.[32-35] Nucleofector kit V was obtained from Amaxa (Gaithersburg, MD). A plasmid containing full-length human Nur77 cDNA was obtained from Origene (Rockville, MD) and the Nur77 open reading frame was polymerase chain reaction (PCR) amplified with primers containing an in-frame N-terminal FLAG tag using *pfu* ultra polymerase (Stratagene, La Jolla, CA). The resulting PCR product was digested with appropriate restriction enzymes and inserted into pcDNA3.1 (Invitrogen, Carlsbad, CA). The sequence and orientation of the cDNA were confirmed by sequencing.

Cell lines and cell culture

CTCL cell lines, HH, HuT-78, and MJ were obtained from ATCC (Manassas, VA). HH cells were grown in RPMI 1640 medium supplemented with 10% FBS, 1% penicillin/streptomycin, and 1% NEAA. HuT-78 cells were cultured in IMDM medium supplemented with 20% FBS. MJ cells were cultured in IMDM supplemented with 10% FBS, 1% penicillin/streptomycin, 1% nonessential amino acids, and IL-2. All cells were passaged 2 to 3 times a week. Exponentially growing cells were used for experiments.

Primary CTCL cells

Primary CTCL cells were obtained with informed consent, in accordance with the Declaration of Helsinki, as part of a clinical protocol approved by the Human Assurance Committee of the Medical College of Georgia. Peripheral blood from CTCL patients was collected in heparinized tubes, and mononuclear cells were separated using Lymphoprep (Axis-Shield, Oslo, Norway), washed once with complete RPMI 1640 media, and resuspended in complete RPMI 1640. $CD4^+$ T cells were isolated from mononuclear cells with a kit from StemCell Technologies (Vancouver, BC). Banked, delinked, and deidentified, donor peripheral blood $CD34^+$ mononuclear cells were purified by immunomagnetic beads conjugated with anti-CD34 antibody before use in the cell viability assay (StemCell Technologies).

Confocal microscopy

HH cells were cultured in the presence or absence of panobinostat for 4 hours. MitoTracker (Invitrogen, Carlsbad, CA) was added to the media to stain mitochondria and the cells were incubated for an additional 30 minutes. Cells were cytospun and stained with anti-Nur77, before performing confocal microscopy, as previously described.[36]

Assessment of apoptosis and synergism

Untreated or drug-treated cells were fixed with 70% ethanol then stained with annexin V and propidium iodide (PI). The percentage of apoptotic cells was determined by flow cytometry as previously described.[37] To analyze synergism between panobinostat and ABT-737 in inducing apoptosis, cells were treated with panobinostat (10-100 nM) and ABT737 (0.1-1.0 μM) at a constant ratio of 1:10 for 48 hours. The percentage of apoptotic cells was determined by flow cytometry as previously described.[37] The combination index (CI) for each drug combination was obtained using the commercially available software Calcusyn (Biosoft, Ferguson, MO).[38] CI values of less than 1.0 represent synergism of the 2 drugs in the combination.

Assessment of percentage nonviable cells

After designated treatments, primary CTCL cells or normal $CD4^+$ T cells were stained with trypan blue (Sigma-Aldrich). The numbers of nonviable cells were determined by counting the cells that showed trypan blue uptake in a hemocytometer, and reported as percentage of untreated control cells.

RNA isolation and reverse-transcription PCR

Total RNA was isolated from cells with an RNeasy mini kit from QIAGEN (Valencia, CA) following the manufacturer's instructions and converted into cDNA using the Superscript II first-strand synthesis kit (Invitrogen). Primers for amplification of Nur77, Nor1, TRAIL, and FasL are listed in Table S1, available on the *Blood* website; see the Supplemental Materials link at the top of the online article. Amplified products were resolved on a 2% agarose gel and recorded with a UV transilluminator. Horizontal scanning densitometry was performed with ImageQuant 5.2 (Amersham Biosciences/GE Healthcare, Piscataway, NJ) and the band intensity of each PCR product was normalized to that of β-actin bands.

Chromatin immunoprecipitation and PCR

Approximately 12×10^6 HH cells were treated with vehicle or 40 nM panobinostat for 4 hours. The chromatin was cross-linked with formaldehyde then cell lysis, sonication, and chromatin immunoprecipitation were performed according to the EZ ChIP manufacturer's protocol (Upstate Biotechnologies, Charlottesville, VA) using rabbit HDAC7 antibody (H237), as previously described[32] (Santa Cruz Biotechnology). The primer sequences for amplification of the Nur77 and Nor1 promoters are listed in Table S1. PCR amplification and resolution of bands were performed, as described in "RNA isolation and reverse-transcription PCR."

Cell lysis and protein quantitation

Untreated or drug-treated cells were harvested and cell pellets were washed with 1× PBS, then lysed and quantitated as previously described.[33,34]

SDS-PAGE and Western blotting

One hundred micrograms of total cell lysate was used for SDS–polyacrylamide gel electrophoresis (PAGE). Western blot analyses of Nur77, HDAC7, Bax, Bak, Bim, Bcl-2, Bcl-x_L, XIAP, acetylated α-tubulin, and PARP were performed on total cell lysates using specific antisera or monoclonal antibodies as previously described.[33,34] The expression level of either β-actin or α-tubulin was used as the loading control for the Western blots. Blots were developed with a chemiluminescent substrate enhanced chemiluminescence (ECL; Amersham Biosciences, Piscataway, NJ).

In vitro HDAC7 activity and immunoprecipitation of HDAC7

Recombinant human HDAC7 (50007; BPS Bioscience, San Diego, CA) was assayed for deacetylase activity using a HDAC fluorimetric cellular activity assay kit following the manufacturer's protocol (AK-503; BIOMOL Research Laboratories, Plymouth Meeting, PA). For in vivo HDAC7 deacetylase activity, HH cells were seeded at 10^5 cells/well in a 6-well plate, cultured overnight, and transfected with FLAG-HDAC7 plasmid (3 μg total DNA) with Lipofectamine 2000 (Invitrogen). After a 48-hour incubation, the cells were washed in 1× PBS and resuspended in cell lysis buffer. For immunoprecipitation, 600 μg total cell

lysate was incubated with 6 μL anti-FLAG M2 antibody (Sigma-Aldrich) for 1 hour at 4°C, then protein G beads were added and the tubes were incubated overnight at 4°C. The immunoprecipitates were washed 4 times with lysis buffer, once with HDAC assay buffer, and resuspended in 600 μL HDAC assay buffer and assayed.

RNA interference of Nur77 and HDAC7

To determine the effects of knockdown of Nur77 and Nor1 in CTCL cells, siRNA duplex oligo for Nur77 was custom synthesized by Ambion (Austin, TX) based on the sequence as described by Lin et al.[24] A predesigned siRNA oligo targeting human HDAC7 was purchased from QIAGEN (catalog no.: si027777726). For depletion of Nor1, a siGENOME SMART-pool was obtained from Dharmacon (Lafayette, CO). Negative control siRNA was obtained from Ambion. All siRNA transfections in HH cells were done using the Amaxa Nucleofector system with Kit V and program O-12. Immediately after nucleofection, cells were placed at a concentration of 10^6/mL in media containing 20% FBS and incubated at 37°C overnight. The next day cells were centrifuged and replated for experimentation.

In vivo model of CTCL

HH cells (10 million) were injected into the flank of female athymic nude mice. Alternatively, HH cells were injected into the lateral tail vein of female athymic nude mice and the mice were monitored for 28 days. Treatment with panobinostat (10 mg/kg and 20 mg/kg) was initiated in the flank tumor model when the average tumor size in all groups was 100 mm^3 (n = 8 mice per group). In the tail vein model, treatment with vehicle or 20 mg/kg panobinostat (n = 10) was initiated on day 29 and administered 3 days a week for 4 weeks. Tumor volume was measured regularly with external calipers to monitor tumor growth. Treatment was withdrawn after 4 weeks in both models. The survival of mice from the tail vein model is represented with a Kaplan-Meier survival plot. Approval for the use of mice in this study was granted by the Medical College of Georgia.

Statistical analysis

Significant differences between values obtained in a population of leukemic cells treated with different experimental conditions were determined using the Student *t* test. *P* values of less than .05 were assigned significance.

Results

Effect of panobinostat on the expression of proapoptotic and antiapoptotic proteins in panobinostat-sensitive and -resistant human CTCL cells

In a previous report Zhang et al had demonstrated that vorinostat selectively induces apoptosis of CTCL cells.[39] In the present studies, we first determined the apoptotic effects of panobinostat in the human CTCL HH, HuT78, and MJ cells. Figure 1A demonstrates that exposure to panobinostat induces dose-dependent apoptosis in all 3 cell lines. The inset shows that exposure to panobinostat also induced caspase-dependent cleavage of PARP in conjunction with apoptosis of HH cells. This was also seen in HuT78 cells (Figure S1A). In contrast to HH and HuT78 cells, MJ cells were relatively resistant to panobinostat-induced apoptosis (Figure 1A). Next, we determined the levels of Bcl-2 family members in HH and MJ cells. Compared with the panobinostat-sensitive HH cells, MJ cells express higher levels of antiapoptotic Bcl-2 and Bcl-x_L but similar levels of Mcl-1 and XIAP. There was also no difference in the expression of the proapoptotic Bax and Bak, whereas Bim was not induced in either HH or MJ cells (Figure 1B and data not shown). In HH versus MJ cells, treatment with panobinostat depleted the levels of the antiapoptotic proteins Bcl-X_L, Mcl-1, and XIAP, while modestly inducing the proapoptotic proteins Bak and Bim in HH cells in a dose- and time-dependent manner (Figure 1B; Figure S1B,C). Similar effects were also observed after treatment with panobinostat in the panobinostat-sensitive HuT78 cells (Figure S1C). Levels and activity of the signal transducer and activator of transcription (STAT) family of proteins have been recently correlated with resistance to HDAC inhibitors in CTCL cells.[40] Therefore, we determined the effects of panobinostat treatment on the levels of unphosphorylated and tyrosine phosphorylated (p) forms of STAT1, STAT3, and STAT5 proteins in MJ and HH cells. MJ but not HH cells expressed p-STAT1, p-STAT3, and p-STAT5, as well as expressed higher levels of STAT1, STAT3, and STAT5. Exposure to only the higher concentrations of panobinostat (40 nM) attenuated the levels of p-STAT1, p-STAT3, and p-STAT5 in the MJ cells (Figure 1C).

Treatment with panobinostat inhibits in vivo CTCL tumor growth and improves survival of nude mice with CTCL cell xenografts

We next determined the in vivo growth inhibitory effects of panobinostat, using the nude mice xenograft model of HH cells, where the HH cells were either implanted subcutaneously in the flank or injected into the tail vein. Effect of panobinostat was evaluated on the growth of cutaneous/subcutaneous lesions in this mouse model. Treatment with panobinostat (20 mg/kg for 4 weeks started 12 days after implantation of HH cells) significantly inhibited the growth of the xenografts (Figure 2A). A lower dose of panobinostat (10 mg/kg) was also initially effective, but exhibited eventual loss of control on tumor growth. In addition, a significant improvement in survival was observed after treatment of mice with established tumors with 20 mg/kg panobinostat for 4 weeks, started 4 weeks after the tail vein injection of HH cells ($P < .05$; Figure 2B). At this dose level, neither a significant weight loss nor any other toxicity was observed over a period of 90 days of treatment with panobinostat (data not shown).

Panobinostat inhibits the levels and activity of HDAC7 both in vitro and in vivo

We next determined the effect of panobinostat on the levels and activity of HDAC7. Treatment with panobinostat (10 to 40 nM) dose-dependently depleted the mRNA and protein levels of HDAC7 in HH cells (Figure 3A). In contrast, panobinostat only modestly reduced HDAC7 mRNA and protein levels in MJ cells (Figure 3A). Panobinostat-mediated depletion of HDAC7 was associated with induction of *Nur77* and *Nor1* mRNA expression in HH cells. This was observed to a lesser extent in MJ cells (Figure 3A top panel). Panobinostat treatment dose- and time-dependently increased the expression of Nur77 protein, again more in HH compared with MJ cells (Figure 3A bottom panel; Figure S2A). Panobinostat also depleted the mRNA of HDAC7 with concomitant increase in *Nur77* and *Nor1* mRNA expression in the panobinostat-sensitive HuT78 CTCL cells (Figure S2B). Due to unavailability of a Nor1-specific antibody, we were unable to assess the effects of panobinostat on the protein expression of Nor1. Exposure to panobinostat (5-50 nM) dose-dependently inhibited the in vitro activity of recombinant HDAC7 in a cell-free assay (Figure 3B). Next, HH cells were transfected with pcDNA/FLAG-HDAC7 and immunoprecipitates of HDAC7 were obtained using anti-FLAG antibody. Treatment of the immunoprecipitates with panobinostat dose-dependently inhibited the activity of HDAC7 (Figure 3C).

Panobinostat depletes HDAC7 occupancy at the Nur77 and Nor1 promoters and induces nuclear export and mitochondrial localization of Nur77 in CTCL cells

HDAC7 is known to be recruited to the promoter of Nur77 upstream of its transcriptional start site, which represses Nur77.[13-15] Chromatin

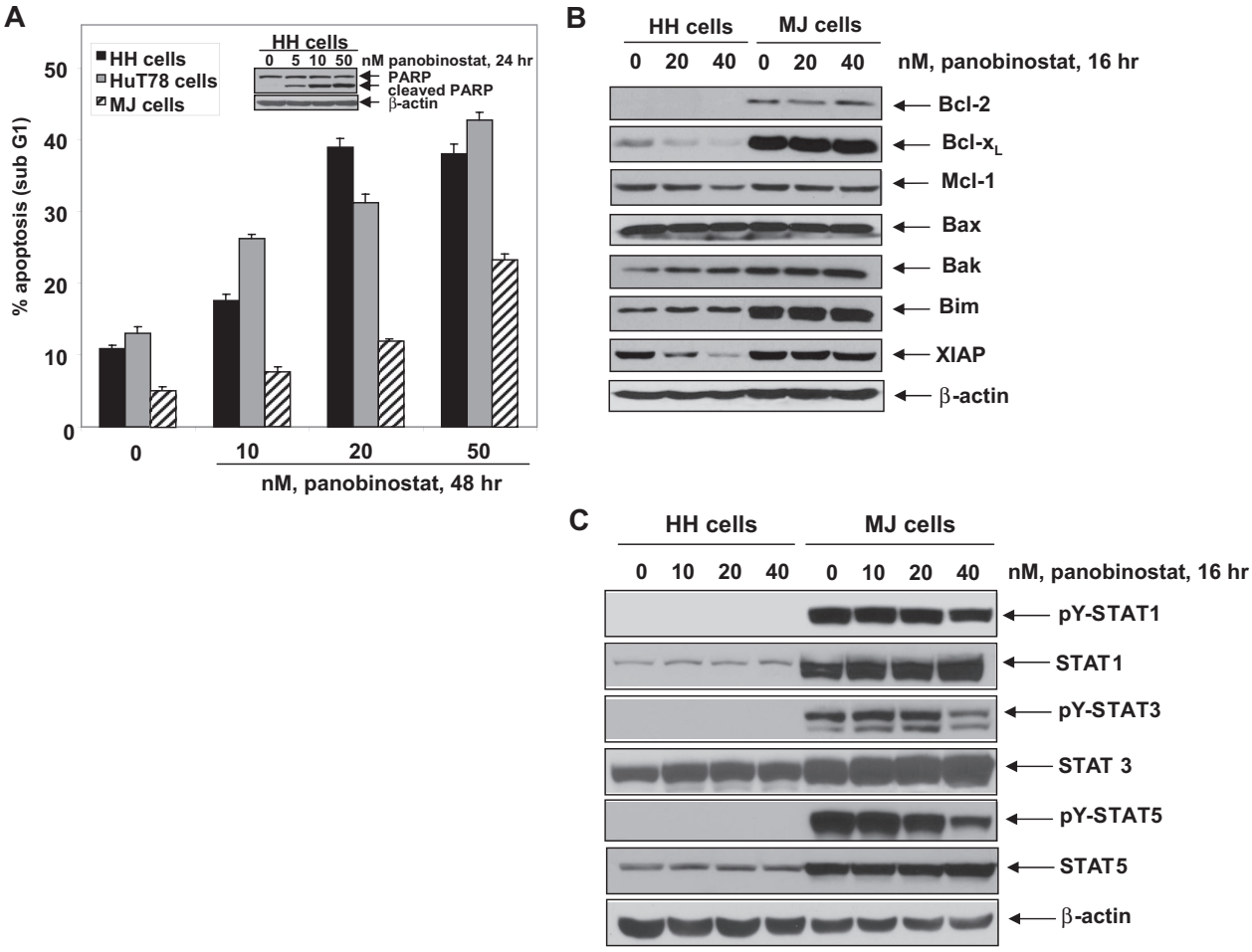

Figure 1. Effect of panobinostat on apoptosis regulators and apoptosis in cultured CTCL cells. (A) HH, HuT78, and MJ cells were treated with the indicated concentrations of panobinostat for 48 hours. Then, apoptosis was determined by flow cytometry. Columns represent mean of 3 experiments; bars, SEM. Inset: Representative Western blot of PARP cleavage from HH cells. (B) HH and MJ cells were treated with the indicated concentrations of panobinostat for 16 hours. Following this, cell lysates were prepared and immunoblot analysis was done for Bcl-2, Bcl-X_L, Mcl-1, Bax, Bak, Bim, and XIAP. The levels of β-actin in the lysates served as the loading control. (C) HH and MJ cells were treated with the indicated concentrations of panobinostat for 16 hours. Following this, total cell lysates were prepared and immunoblot analysis was done for tyrosine-phosphorylated STAT1, STAT3, and STAT5. Blots were stripped and reprobed for total levels of STAT1, STAT3, and STAT5. The expression of β-actin in the lysates served as the loading control.

immunoprecipitates (ChIPs) using anti-HDAC7 antibody demonstrated that, in HH cells, treatment with panobinostat for 4 hours also decreased the binding of HDAC7 to the promoter of Nur77 and Nor1 by approximately 40% and 70%, respectively (Figure 4A). There was no significant difference in the input DNA from untreated and panobinostat-treated cells. We also determined whether treatment with decitabine would induce *Nur77* and *Nor1* mRNA, thereby indicating the involvement of DNA methyltransferase 1 (DNMT1) in the transcriptional activation of Nur77 and Nor1 promoters. As shown in Figure 4B, neither treatment with decitabine alone nor cotreatment with decitabine and panobinostat augmented *Nur77* and *Nor1* mRNA levels in HH cells. We next determined the effect of panobinostat treatment on the subcellular localization of Nur77 in CTCL cells. HH cells were treated with panobinostat for 4 hours, followed by staining with MitoTracker and/or anti-Nur77 antibody and analysis with confocal immunofluorescent microscopy. As demonstrated in Figure 4C, treatment with panobinostat significantly increased the cytoplasmic staining of Nur77, as well as its colocalization with the MitoTracker, indicating translocation of Nur77 to the mitochondria. This was followed by caspase activation and apoptosis, as above (Figure 1). Next, we determined the mechanistic link between HDAC7 depletion and Nur77 induction in CTCL cells. We transfected siRNA to HDAC7 or Nur77 into HH cells. As shown in Figure 4D, siRNA to HDAC7 attenuated *HDAC7* mRNA by 70%, which resulted in a 1.7-fold increase in the mRNA levels of Nur77. Conversely, siRNA-mediated depletion of Nur77 did not affect *HDAC7* mRNA levels in HH cells (Figure 4D). We next determined whether knockdown of HDAC7 by siRNA would decrease HH cell viability. HH cells were transfected with either control or HDAC7 siRNA and the down-regulation of HDAC7 was assessed 48 hours after transfection (Figure S3A) and cell viability was determined 96 hours after transfection. Compared with control siRNA–transfected cells, siHDAC7-transfected cells exhibited slightly increased loss of cell viability (Figure S3B).

Overexpression of Nur77 increases whereas depletion of Nur77 and Nor1 by RNA interference significantly inhibits panobinostat-mediated apoptosis of cultured CTCL cells

We next determined the effects of ectopic overexpression of Nur77 on the viability and sensitivity of HH cells to panobinostat. HH cells were transfected with empty vector or Nur77 cDNA for 48 hours. Following this, reverse-transcription (RT)–PCR and immunoblot analyses were performed. Compared with HH cells transfected with the empty vector, a markedly increased expression of Nur77 was observed in cells transfected with Nur77 (Figure 5A).

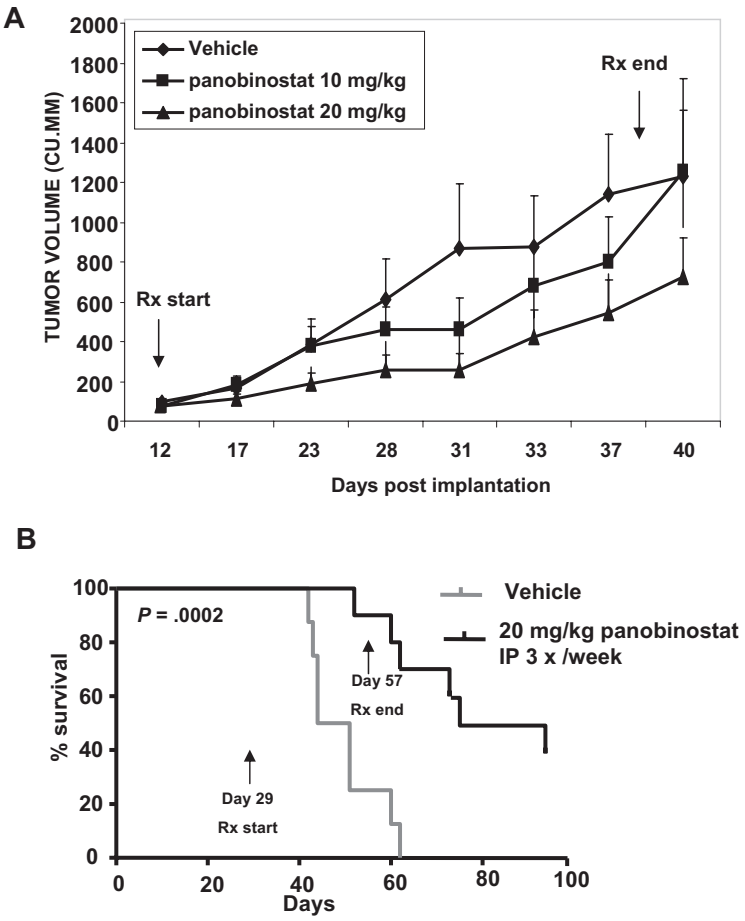

Figure 2. Treatment with panobinostat causes significant tumor growth delay and prolongs survival of mice implanted with CTCL cells. (A) HH cells were injected into the flank of female athymic nude mice. Treatment began when tumors were approximately 100 mm^3. Mice were treated intraperitoneally with DMSO, or 10 mg/kg or 20 mg/kg panobinostat 3 days per week for 4 weeks. n = 8 per group. Mean tumor volumes ± SEM are shown. (B) Female athymic nude mice were injected in the lateral tail vein with HH cells. The cells were allowed to engraft for 28 days before initiation of treatment. Mice were treated intraperitoneally with DMSO or 20 mg/kg panobinostat 3 days per week for 4 weeks. n = 10 per group. Survival of the mice in both groups (vehicle and panobinostat) is represented by Kaplan-Meier plot.

Notably, ectopic overexpression of Nur77 not only induced apoptosis but also further sensitized HH cells to panobinostat-induced apoptosis (Figure 5B). In HH cells, we did not find induction of FasL or TRAIL mRNA, after treatment with panobinostat for 4 hours (Figure S4A). In addition, ectopic overexpression of Nur77 did not induce *TRAIL* or *FasL* mRNA expression in HH cells (Figure S4B). Collectively, these data suggest that the mitochondria-based Nur77-mediated proapoptotic mechanism could potentially lower the threshold and sensitize CTCL cells to panobinostat-induced apoptosis. We next determined the effects of knockdown of Nur77 and/or Nor1 on panobinostat-induced apoptosis. Transfection of siRNA to Nur77 or Nor1 inhibited panobinostat-induced mRNA of Nur77 or Nor1, respectively, in HH cells (data not shown). However, the knockdown of *Nur77* or *Nor1* mRNA alone did not significantly affect panobinostat-induced apoptosis of HH cells (data not shown). Compared with the cells transfected with the control siRNAs, cotransfection with the Nur77 and Nor1 siRNAs resulted in a significant inhibition of panobinostat-induced mRNA expression of Nur77 and Nor1 (Figure 5C). Furthermore, abrogation of *Nur77* and *Nor1* mRNA induction by cotransfection with siRNAs to Nur77 and Nor1 significantly inhibited panobinostat-induced apoptosis of HH cells (Figure 5D). This was especially evident after treatment of HH cells with relatively low concentrations of panobinostat (10 and 20 nM) ($P = .04$ and $P = .01$, respectively). Apoptosis induced by higher concentrations of panobinostat (40 nM) was less inhibited after combined knockdown of Nur77 and Nor1 (data not shown). Collectively, these data suggest that the mitochondria-based Nur77-mediated proapoptotic mechanism could potentially lower the threshold and sensitize CTCL cells to panobinostat-induced apoptosis.

Cotreatment with ABT-737 synergistically enhanced panobinostat-induced apoptosis of CTCL cells

Because ectopic overexpression of Nur77 sensitized CTCL cells to panobinostat, we next determined the effects of cotreatment with ABT-737 on the activity of panobinostat against HH and MJ cells. Treatment with panobinostat alone induced PARP cleavage more in HH than MJ cells, whereas ABT-737 treatment alone increased PARP cleavage both in HH and MJ cells (Figure 6A). In addition, cotreatment with ABT-737 augmented panobinostat-mediated PARP cleavage in both HH and MJ cells (Figure 6A). Consistent with this, cotreatment with ABT-737 also significantly enhanced panobinostat-induced apoptosis of HH and MJ cells, as determined with annexin/PI staining and flow cytometry (Figure 6B,C). Notably, compared with HH, cotreatment with ABT-737 did not sensitize $CD34^+$ normal bone marrow progenitor cells to panobinostat (Figure 6B). Combined treatment with ABT-737 (dose range 100-1000 nM) and panobinostat (10-100 nM) synergistically induced apoptosis in both HH and MJ cells, as determined by median dose effect analysis.[38] Combination indices for the 2 agents in both cell lines were less than 1.0, indicating synergistic effects (Figure 6D).

Panobinostat depletes HDAC7, induces the expression and nuclear export of Nur77, and induces loss of viability of primary CTCL cells

We next determined the effects of panobinostat treatment on primary CTCL cells. Treatment with panobinostat or vorinostat dose-dependently caused loss of cell viability in primary CTCL cells derived from 5 patients with advanced CTCL (Figure 7A). We

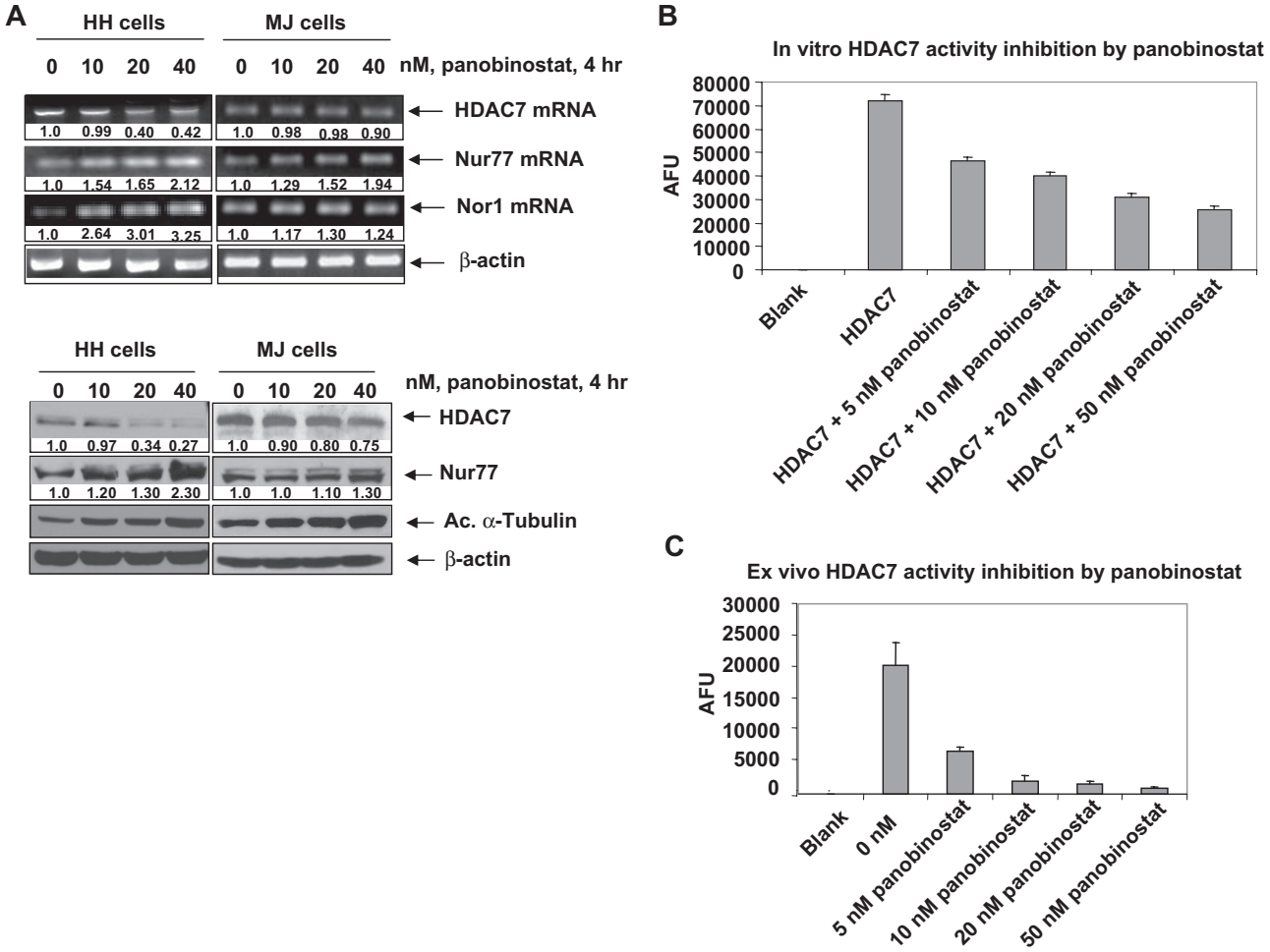

Figure 3. Panobinostat inhibits the levels and activity of HDAC7 as well as induces Nur77 and Nor1 levels. (A) HH and MJ cells were treated with the indicated concentrations of panobinostat for 4 hours. Following this, total RNA was isolated and RT-PCR was done for HDAC7, Nur77, and Nor1. A β-actin–specific PCR and expression served as the loading control for the amplification. Alternatively, after treatment with panobinostat, total cell lysates were isolated and immunoblot analysis was done for HDAC7, Nur77, and acetylated α-tubulin. The levels of β-actin in the cell lysates served as the loading control. (B) Recombinant HDAC7 (3.6 μg protein/well) was incubated at 37°C with 100 μM Fluor de Lys substrate (BIOMOL Research Laboratories, Plymouth Meeting, PA) and indicated concentrations of panobinostat (0, 5, 10, 20, and 50 nM) for 1 hour in the assay buffer provided by the manufacturer. Reactions were stopped with Fluor de Lys developer and fluorescence was measured (CytoFluor II; PerSeptive Biosystems [BioTek Instruments, Winooski, VT]; excitation: 360 nm, emission: 460 nm). Experiment was performed in triplicate and the value of the blank was deducted from all experimental values. (C) FLAG-tagged HDAC7 was immunoprecipitated from untreated HH cells. Fifteen micrograms (1 μg/μL) HDAC7 immunoprecipitate was incubated at 37°C with 100 μM Fluor de Lys substrate and indicated concentrations of panobinostat for 1 hour in the assay buffer provided by the manufacturer. Reactions were stopped with Fluor de Lys developer and fluorescence was measured (CytoFluor II; excitation: 360 nm, emission: 460 nm). The value of the blank was deducted from all experimental values. Values represent the mean ± SEM of 3 experiments.

also determined the effects of panobinostat and vorinostat treatment on normal $CD4^+$ T cells. Panobinostat and vorinostat treatment exhibited very low cytotoxicity against normal $CD4^+$ T cells and induced less than 15% cell death at 20 nM and 2 μM, respectively (Figure 7B). We also determined the effect of in vivo treatment with panobinostat on HDAC7 and Nur77 in the patient-derived circulating CTCL cells in the peripheral blood. Compared with the pretreatment CTCL cells, circulating CTCL cells, isolated from the peripheral blood 6 hours after the first oral administration of 20 mg panobinostat to the patient with advanced CTCL, showed attenuation of HDAC7 and induction of Nur77 levels (Figure 7C). Furthermore, this was associated with increased cytosolic and mitochondrial localization of Nur77; the latter was demonstrated by colocalization of Nur77 with the Mitrotracker, as determined by confocal immunofluorescent microscopy (Figure 7D). These effects were also seen after ex vivo treatment of primary CTCL cells with panobinostat (data not shown). Collectively, these findings mimicked those that were observed after in vitro treatment of cultured CTCL cells with panobinostat (Figures 3A and 4C, and data not shown).

Discussion

Although treatment with HDIs has yielded some clinical benefit in other hematologic malignancies, for example, Hodgkin disease and non-Hodgkin lymphoma (NHL),[9] these agents have been clinically most effective against CTCL.[4-9] Data presented here provide an explanation for the relatively higher sensitivity of CTCL cells to HDIs, for example, panobinostat, as well as elucidate a targeting strategy for the mechanism(s) that confers relative resistance to HDIs in CTCL cells. Panobinostat is well documented to have low nanomolar activity against class I and II HDACs.[34] In addition, it has been shown to lower both the levels and activity of HDAC7.[12,41] Our findings unequivocally demonstrate that, by attenuating HDAC7, which results in

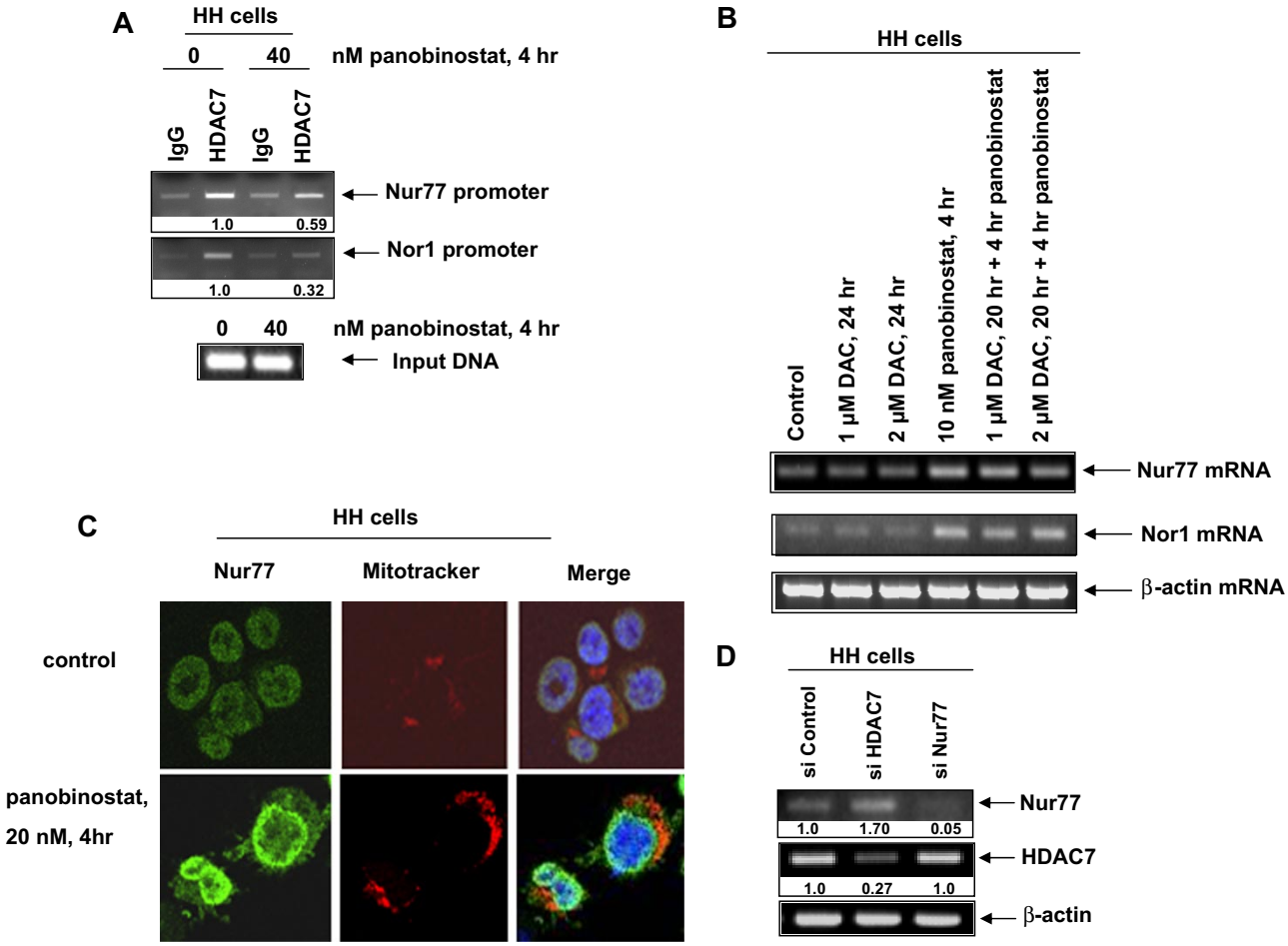

Figure 4. Treatment with panobinostat enhances transcription of Nur77 or Nor1 by depleting HDAC7 occupancy at the Nur77 and Nor1 promoters. (A) HH cells were treated with the indicated concentrations of panobinostat for 4 hours. After treatment, chromatin immunoprecipitations were performed for HDAC7 and the immunoprecipitated chromatin and sonicated chromatin inputs were PCR amplified for the Nur77 and Nor1 promoters. (B) HH cells were treated with the indicated concentrations of decitabine (DAC) and panobinostat for 4 to 24 hours. Then, cells were harvested and total RNA was extracted and RT-PCR was done for Nur77 and Nor1. A β-actin–specific PCR and expression served as the loading control for the amplification. (C) HH cells were treated with the indicated concentrations of panobinostat for 4 hours. Thirty minutes before the end of the incubation, MitoTracker was added to stain mitochondria. Then, the cells were cytospun onto glass slides, fixed, permeabilized, and stained for Nur77. Images were acquired with a Zeiss LSM510 meta confocal microscope (Carl Zeiss, Heidelberg, Germany) equipped with a 63×/1.2 NA water immersion–objective lens. (D) HH cells were transfected with control siRNA or siRNA directed against HDAC7 and Nur77, respectively, for 48 hours. Following this, RT-PCR was done for HDAC7 and Nur77. A β-actin–specific PCR and expression served as the loading control for the amplification.

derepression of the prodeath nuclear orphan receptors Nur77 and Nor1, panobinostat induces the levels and mitochondrial translocation of Nur77 and Nor1 as well as triggers apoptosis of CTCL cells.[14] These observations establish that HDAC7-Nur77–based mechanism is involved in the lethal action of panobinostat against CTCL cells. Although panobinostat-mediated depletion of HDAC7 was mechanistically linked to attenuation of HDAC7 mRNA, what remained unclear is how panobinostat depletes the mRNA levels of HDAC7. We had previously reported that HDIs activate caspase-8 in acute myeloid leukemia (AML) cells.[32] Recently, HDAC7 was shown to be more rapidly and more efficiently cleaved by caspase-8 than any other currently known caspase-8 substrates.[42] Whether panobinostat-mediated activation of caspase-8 is responsible for depletion of the levels and activity of HDAC7 protein was not specifically addressed in the present studies. Regardless, depletion of HDAC7 by panobinostat treatment resulted in decreased recruitment of HDAC7 to the promoter region of Nur77 and Nor1. This resulted in derepression of Nur77 and Nor1. These findings were observed in both cultured and primary CTCL cells. Notably, ex vivo treatment with panobinostat of CTCL cells, isolated from the peripheral blood of 5 patients, also exhibited dose-dependent increase in loss of cell viability, while demonstrating low cytotoxicity against normal $CD4^+$ T cells. In one of these patients with advanced CTCL, who was also enrolled in a clinical trial in which the patient received panobinostat 20 mg orally 3 times per week, treatment with panobinostat also caused in vivo depletion of HDAC7, as well as induction and translocation of Nur77 to the mitochondria. These findings raise the possibility that in vivo treatment with panobinostat may also eliminate CTCL cells in patients by engaging the HDAC7-Nur77–based mechanism. It is also clear from our findings that panobinostat treatment may also be mediating apoptosis of CTCL cells through other non-HDAC7–dependent mechanisms. It is possible that HDAC7 is just one of the links between panobinostat mediated up-regulation of Nur77/Nor1, and HDAC7 attenuation is essential but not sufficient for panobinostat-mediated induction and mitochondria translocation of Nur77 and Nor1. Consistent with this, our data (presented in Figure S3) show that knockdown of HDAC7 by siRNA only slightly induces apoptosis of CTCL cells. It is also well documented that Nur77 protein undergoes extensive posttranscriptional modifications. Therefore, it will be

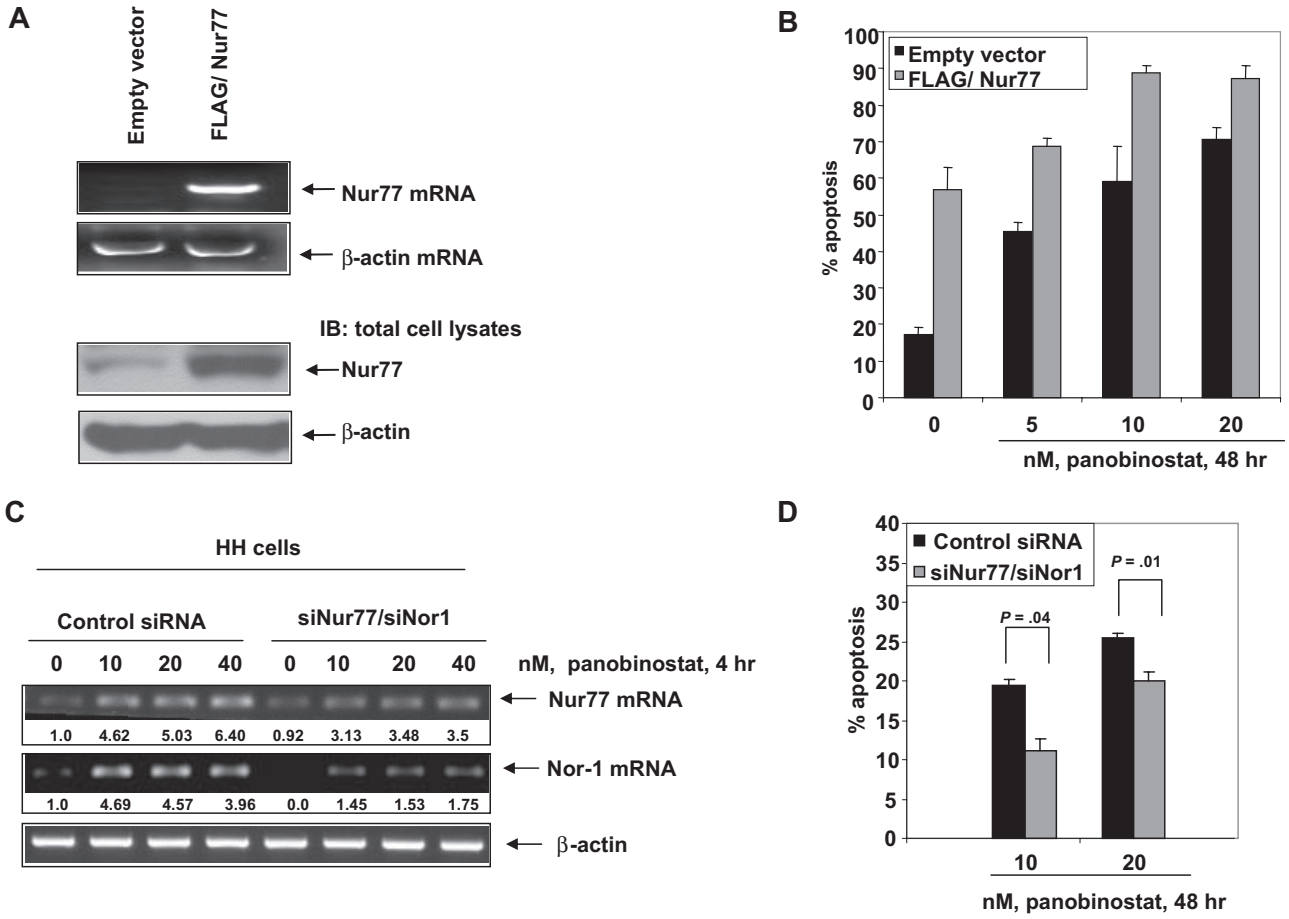

Figure 5. Overexpression of Nur77 enhances panobinostat-induced apoptosis, whereas combined RNA interference of Nur77 and Nor1 decreases panobinostat sensitivity of CTCL cells. (A) HH cells were transfected with empty vector or pcDNA3.1 FLAG/Nur77 for 48 hours. Then, total RNA was isolated and RT-PCR was done for Nur77. A β-actin–specific PCR and expression served as the loading control for the amplification. Alternatively, total cell lysates were prepared and immunoblot analysis was done for Nur77. The levels of β-actin in the lysates served as the loading control. (B) HH cells were transfected with empty vector or pcDNA3.1 FLAG/Nur77 for 48 hours. Transfected cells were treated with the indicated concentrations of panobinostat for 48 hours. Apoptosis was assessed by staining with propidium iodide and subG1 cells were detected by flow cytometry. Columns represent mean of 3 experiments; bars, standard error of the mean. (C) HH cells were transfected with control siRNA or siNur77 and siNor1 for 48 hours. Following this, the cells were treated with the indicated concentrations of panobinostat for 4 hours and RT-PCR was done for Nur77 and Nor1. A β-actin–specific PCR and expression served as the loading control for the amplification. (D) HH cells were transfected with control siRNA or siNur77 and siNor1 for 48 hours. Following this, transfectants were treated with the indicated concentrations of panobinostat for 48 hours and apoptosis was assessed by flow cytometry. Columns represent mean of 3 experiments; bars, standard error of the mean. Statistical significance was determined by Student *t* test.

interesting to determine in the future whether panobinostat can induce any known or novel modifications of Nur77 protein posttranscriptionally.

To elucidate potential mechanisms of resistance to panobinostat activity against CTCL cells, we compared panobinostat-sensitive HH versus panobinostat-resistant MJ cells. Our findings demonstrate that panobinostat treatment caused more depletion of HDAC7 and induced more Nur77 and Nor1 in HH versus MJ cells. This could be explained by the observation that, after panobinostat treatment, more HDAC7 remained in the nucleus to bind to the promoters of Nur77 and Nor1 and inhibit their expressions in MJ cells. This could potentially contribute to the resistance of MJ cells to panobinostat. There is emerging evidence that by depleting the levels of the histone H3-K27 methyltransferase EZH2 and disrupting the polycomb repressive complex 2 (PRC2), panobinostat could also disrupt DNMT1-mediated DNA methylation.[43-45] This raised the question whether panobinostat-mediated inhibition of DNMT1 and demethylation of the promoter DNA of Nur77 and Nor1 genes contributed to derepression of Nur77 and Nor1. However, treatment with the DNMT1 inhibitor decitabine did not induce Nur77 and Nor1; making it unlikely that DNA methylation is responsible for their repression in CTCL cells. A previous report had indicated that in cancer cells AKT activity inhibits phosphorylation and nuclear export of Nur77, whereas inhibition of AKT promotes translocation of Nur77 from the nucleus to the cytoplasm.[46] Although not studied here, we have previously shown that panobinostat inhibits AKT activity.[33] To what extent this action of panobinostat is involved in promoting nuclear export of Nur77 remains to determined.[33]

At the mitochondria, binding of Nur77 to the N-terminal loop in the Bcl-2 induces a conformational change that exposes the BH3 domain and converts Bcl-2 from an antiapoptotic to a killer protein.[24] Our findings also show that treatment with panobinostat induced mitochondrial localization of Nur77, which was associated with PARP cleavage activity of caspases and apoptosis of CTCL cells. After treatment with panobinostat, we did not see induction of either TRAIL or FasL mRNA in human CTCL cells. Our findings are consistent with those recently reported, which demonstrated that during negative selection of the $CD4^+$ $CD8^+$ thymocytes Nur77 and Nor1 translocate to the mitochondria, where they associate with Bcl-2 and expose its proapoptotic BH3 domain.[25] If this is the predominant mechanism of prodeath activity of Nur77 and Nor1, it also implies that cells with high Bcl-2 and Bcl-x_L overexpression would be particularly susceptible to the lethal

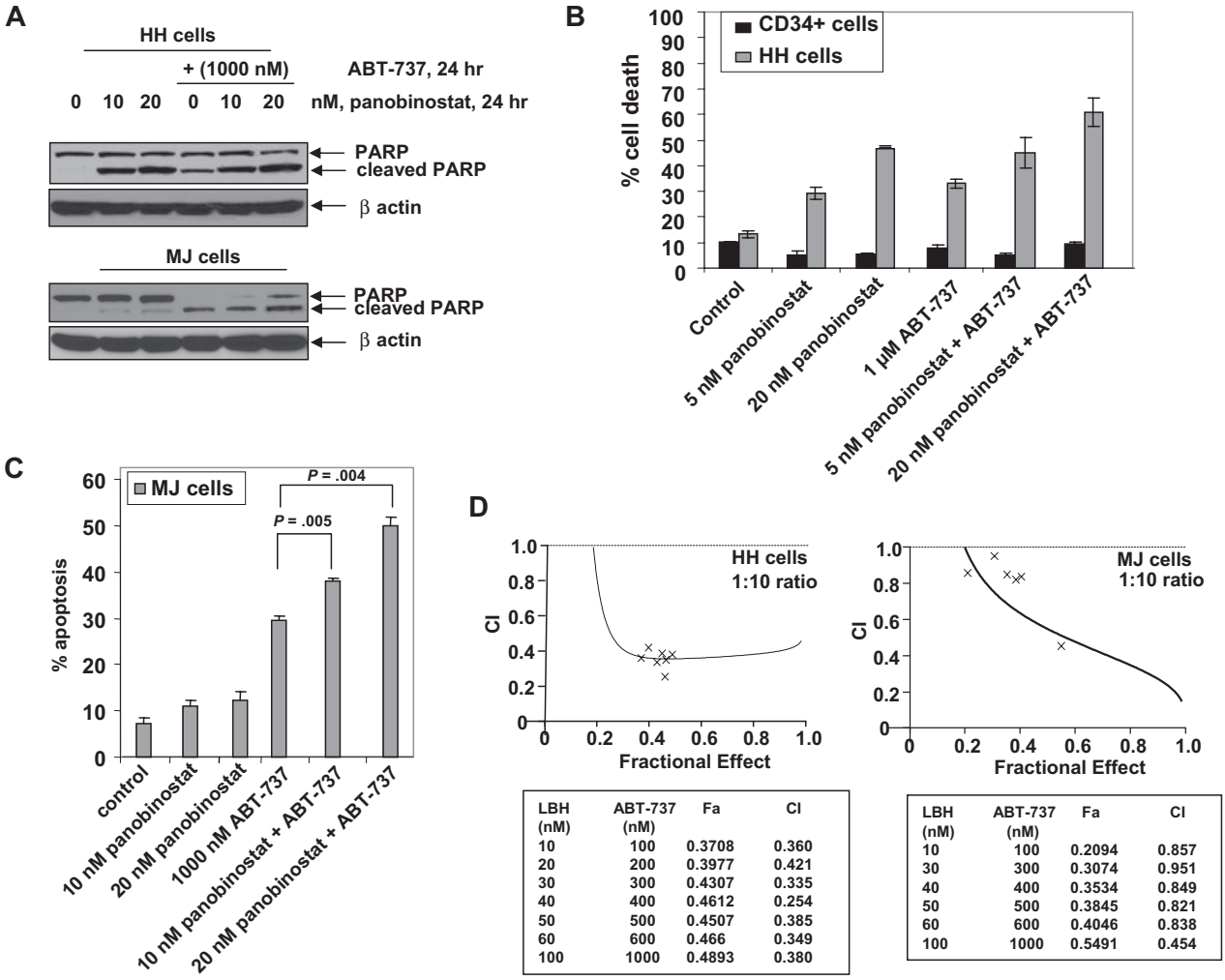

LBH (nM)	ABT-737 (nM)	Fa	CI
10	100	0.3708	0.360
20	200	0.3977	0.421
30	300	0.4307	0.335
40	400	0.4612	0.254
50	500	0.4507	0.385
60	600	0.466	0.349
100	1000	0.4893	0.380

LBH (nM)	ABT-737 (nM)	Fa	CI
10	100	0.2094	0.857
30	300	0.3074	0.951
40	400	0.3534	0.849
50	500	0.3845	0.821
60	600	0.4046	0.838
100	1000	0.5491	0.454

Figure 6. Cotreatment with ABT-737 and panobinostat synergistically induces apoptosis of CTCL cells. (A) HH and MJ cells were treated with panobinostat and/or ABT-737 (1000 nM) for 24 hours. Total cell lysates were prepared and immunoblot analysis was done for cleaved PARP. The levels of β-actin in the lysates served as the loading control. (B) HH and primary normal CD34$^+$ cells were treated with the indicated concentrations of panobinostat and/or ABT-737 for 48 hours. Then, the percentages of nonviable cells were determined by trypan blue dye uptake in a hemocytometer. Values represent the percentage of nonviable cells from each condition compared with untreated cells. Columns represent mean of 3 experiments; bars, standard error of the mean. (C) MJ cells were treated with the indicated concentrations of ABT-737 and panobinostat for 48 hours. Following this, the percentage of apoptotic cells was determined by flow cytometry. Columns represent mean of 3 experiments; bars, standard error of the mean. (D) HH and MJ cells were treated with panobinostat and/or ABT-737 at a fixed ratio of 1 to 10 (with concentrations ranging from 10-100 nM panobinostat) for 48 hours. Then, the percentage of apoptotic cells was determined by flow cytometry. Using Calcusyn software (Biosoft), the analysis of the dose-effect relationship for panobinostat and ABT-737–induced apoptosis of HH or MJ cells was performed according to the median effect equation of Chou and Talalay. The combination index (CI) values were calculated for 3 independent experiments. CI less than 1, CI = 1, and CI more than 1 represent synergism, additivity, and antagonism of the 2 agents, respectively.

outcome of the mitochondrial localization of Nur77 and Nor1.[22-24] However, in colon cancer cells, Nur77-mediated apoptosis was not shown to be due to direct mitochondrial targeting but due to its cytoplasmic translocation, resulting in Bax recruitment to the mitochondria.[47] This suggests that high Bcl-2/Bcl-x_L/Mcl-1 levels would instead inhibit apoptosis secondary to Bax translocation to the mitochondria induced by Nur77 and Nor1. Our findings are consistent with this inference, because panobinostat-resistant MJ versus panobinostat-sensitive HH cells exhibit significantly higher expression of Bcl-2 and Bcl-x_L. Previous studies have also shown that due to blockade of cyctochrome *c* release, apoptosis may be inhibited despite Nur77 targeting of mitochondria.[48] Collectively, these observations suggest that levels and activity of the antiapoptotic proteins, regardless of whether these are antagonized or unaffected by Nur77, govern panobinostat sensitivity of HH versus MJ cells.

In addition to inducing levels and cytoplasmic localization of Nur77, panobinostat treatment has been shown to lower expression and activity of antiapoptotic proteins and induce the levels of prodeath proteins.[33,34] Our findings here show that, in general, treatment with panobinostat lowered the levels of antiapoptotic and increased proapoptotic proteins to a greater extent in HH and HuT78 than in MJ cells. Most likely, this lowered the threshold and enhanced ABT-737–induced apoptosis of HH more than MJ cells. Abrogating Mcl-1 level has been shown to sensitize lymphoma and cancer cells to ABT-737.[31] Because panobinostat treatment lowered Mcl-1 levels only in HH cells, this could be partly responsible for the lower synergistic activity of ABT-737 plus panobinostat against MJ compared with HH cells. It is possible that other potential mechanisms downstream of mitochondria may also confer resistance to panobinostat in MJ cells.[49] This could explain why attenuation of Nur77 and Nor1 could only partially inhibit panobinostat-induced apoptosis in CTCL cells. Compared with HH, MJ cells expressed higher levels of XIAP, which were unaffected by treatment with panobinostat. This may also contribute to the lower sensitivity

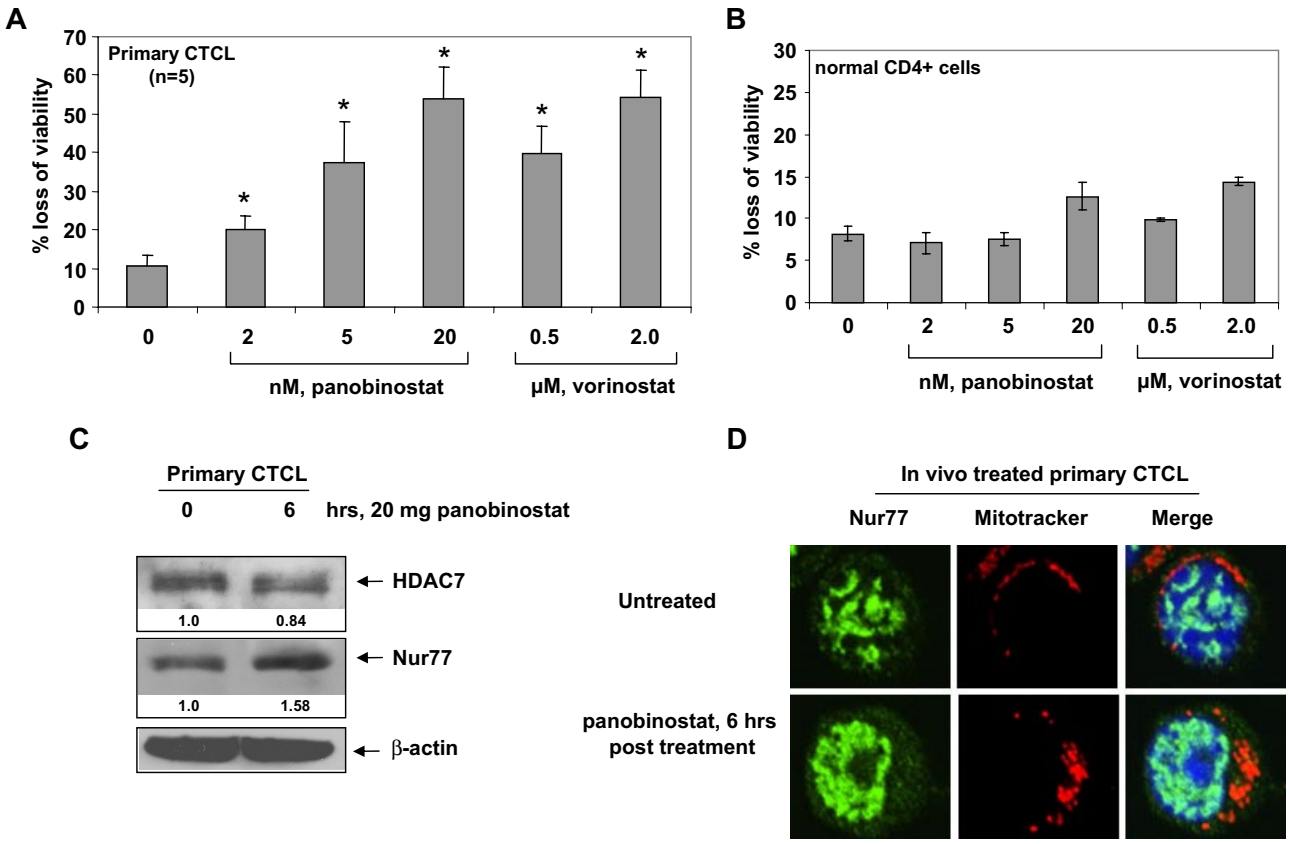

Figure 7. Panobinostat induces expression and mitochondrial localization of Nur77, as well as induces loss of viability of primary CTCL cells. (A) Bone marrow– or peripheral blood–derived $CD4^+$ primary CTCL cells from 5 patients with advanced CTCL were treated with the indicated concentrations of panobinostat or vorinostat for 48 hours. Then, the percentages of nonviable cells were determined by trypan blue dye uptake in a hemocytometer. Values represent the percentage of nonviable cell from each condition compared with untreated cells. * denotes values significantly different from that of untreated controls ($P < .05$). (B) Normal $CD4^+$ cells from peripheral blood were treated with the indicated concentrations of panobinostat or vorinostat for 48 hours. Following this, the percentages of nonviable cells were determined by trypan blue dye uptake in a hemocytometer. Values represent the percentage of nonviable cells from each condition compared with untreated cells. (C) Total cell lysates from $CD4^+$ cells harvested from the peripheral blood of a CTCL patient undergoing panobinostat treatment were prepared and immunoblot analysis was done for HDAC7 and Nur77. The levels of β-actin in the lysates served as the loading control. (D) Primary CTCL cells were harvested from a patient undergoing panobinostat treatment at the indicated times. Cells were incubated with MitoTracker for 30 minutes, cytospun, and stained with Nur77. Images were acquired with a Zeiss LSM510 meta confocal microscope equipped with a 63×/1.2 NA water immersion–objective lens.

of MJ cells to panobinostat and explain the lower level of synergistic activity of the combination of ABT-737 and panobinostat against MJ versus HH cells. As also previously reported, we observed high levels of the unphosphorylated and phosphorylated versions of STAT1, STAT3, and STAT5 in MJ versus HH cells, suggesting that persistent activation of STAT1, STAT3, and STAT5 may contribute to panobinostat resistance in CTCL cells.[40] Only at higher concentrations did panobinostat treatment lower p-STAT3 and p-STAT5 levels in MJ cells. Taken together, these findings underscore that more than one mechanism contributes to the resistance of CTCL cells to panobinostat. Because STAT3 and STAT5 activities have been shown to induce the levels of the antiapoptotic Bcl-2 family members,[50] by abrogating their levels and activities downstream of the activities of STATs, cotreatment with panobinostat and ABT-737 synergistically induces apoptosis of CTCL cells. Whether combining an inhibitor of JAK/STAT activity would add to the synergistic effects of panobinostat plus ABT-737 remains to be determined.

Our findings presented here clearly demonstrate that panobinostat-mediated depletion of HDAC7 with concomitant upregulation and mitochondrial localization of Nur77 also occurred in the circulating CTCL cells after in vivo treatment with panobinostat. Clinical relevance of our findings will have to await implementation of clinical studies of panobinostat and Bcl-2/Bcl-x_L antagonist with correlative studies of the biomarkers highlighted by present studies. ABT-263 is the orally active derivative of ABT-737, which is in early clinical trials in lymphoid malignancies, small-cell lung cancer, and chronic lymphocytic leukemia.[51] The combination of panobinostat and ABT-263 and its correlative predictive biomarker evaluations may also represent a promising future approach for the treatment of other T- or B-cell malignancies where HDAC7-Nur77– and Bcl-2/Bcl-X_L–based mechanisms regulate survival of the malignant cells, for example, NHL and multiple myeloma.

Authorship

Contribution: J.C., W.F., K.E., Y.W., R.R., R.J., Y.Y., R.K., and P.C. performed the in vitro studies with the cultured CTCL cells; P.F., P.L., and R.B. performed the in vivo HH cell xenograft studies in nude mice; K.N. and A.J. procured and assisted in performing the studies on primary CTCL cells; P.A. provided reagents for the study; and K.N.B. planned and supervised the in vitro and in vivo studies and prepared the report.

Conflict-of-interest disclosure: P.A. is an employee of Novartis Institute for Biomedical Research Inc and K.N.B. has received clinical

and laboratory research support from Novartis Institute for Biomedical Research. K.N. and A.J. received research support from Novartis. All other authors declare no competing financial interests.

Correspondence: Kapil Bhalla, MCG Cancer Center, Medical College of Georgia, 1120 15th St, CN-2101 Augusta, GA 30912; e-mail: kbhalla@mcg.edu.

References

1. Willemze R, Jaffe ES, Burg G, et al. WHO-EORTC classification for cutaneous lymphomas. Blood. 2005;105:3768-3785.
2. Querfeld C, Rosen ST, Guitart J, Kuzel TM. The spectrum of cutaneous T-cell lymphomas: new insights into biology and therapy. Curr Opin Hematol. 2005;12:273-278.
3. Kim EJ, Hess S, Richardson SK, et al. Immunopathogenesis and therapy of cutaneous T cell lymphoma. J Clin Invest. 2005;115:798-812.
4. Piekarz RL, Robey R, Sandor V, et al. Inhibitor of histone deacetylation, depsipeptide (FR901228), in the treatment of peripheral and cutaneous T-cell lymphoma: a case report. Blood. 2001;98:2865-2868.
5. Duvic M, Talpur R, Ni X, et al. Phase 2 trial of oral vorinostat (suberoylanilide hydroxamic acid, SAHA) for refractory cutaneous T-cell lymphoma (CTCL). Blood. 2007;109:31-39.
6. Ellis L, Pan Y, Smyth GK, et al. Histone deacetylase inhibitor panobinostat induces clinical responses with associated alterations in gene expression profiles in cutaneous T-cell lymphoma. Clin Cancer Res. 2008;14:4500-4510.
7. Glaser KB. HDAC inhibitors: clinical update and mechanism-based potential. Biochem Pharmacol. 2007;74:659-671.
8. Olsen EA, Kim YH, Kuzel TM, et al. Phase IIb multicenter trial of vorinostat in patients with persistent, progressive, or treatment refractory cutaneous T-cell lymphoma. J Clin Oncol. 2007;25:3109-3115.
9. Mann BS, Johnson JR, He K, et al. Vorinostat for treatment of cutaneous manifestations of advanced primary cutaneous T-cell lymphoma. Clin Cancer Res. 2007;13:2318-2322.
10. Minucci S, Pelicci PG. Histone deacetylase inhibitors and the promise of epigenetic (and more) treatments for cancer. Nat Rev Cancer. 2006;6:38-51.
11. Yang XJ, Seto E. The Rpd3/Hda1 family of lysine deacetylases: from bacteria and yeast to mice and men. Nat Rev Mol Cell Biol. 2008;9:206-218.
12. Dokmanovic M, Perez G, Xu W, et al. Histone deacetylase inhibitors selectively suppress expression of HDAC7. Mol Cancer Ther. 2007;6:2525-2534.
13. Dequiedt F, Kasler H, Fischle W, et al. HDAC7, a thymus-specific class II histone deacetylase, regulates Nur77 transcription and TCR-mediated apoptosis. Immunity. 2003;18:687-698.
14. Dequiedt F, Van Lint J, Lecomte E, et al. Phosphorylation of histone deacetylase 7 by protein kinase D mediates T cell receptor-induced Nur77 expression and apoptosis. J Exp Med. 2005;201:793-804.
15. Kasler HG, Verdin E. Histone deacetylase 7 functions as a key regulator of genes involved in both positive and negative selection of thymocytes. Mol Cell Biol. 2007;27:5184-5200.
16. Parra M, Mahmoudi T, Verdin E. Myosin phosphatase dephosphorylates HDAC7, controls its nucleocytoplasmic shuttling, and inhibits apoptosis in thymocytes. Genes Dev. 2007;21:638-643.
17. Mangelsdorf DJ, Evans RM. The RXR heterodimers and orphan receptors. Cell. 1995;83:841-850.
18. Winoto A, Littman DR. Nuclear hormone receptors in T lymphocytes. Cell. 2002;109(suppl):S57-S66.
19. Shipp MA, Ross KN, Tamayo P, et al. Diffuse large B-cell lymphoma outcome prediction by gene-expression profiling and supervised machine learning. Nat Med. 2002;8:68-74.
20. Rajpal A, Cho YA, Yelent B, et al. Transcriptional activation of known and novel apoptotic pathways by Nur77 orphan steroid receptor. EMBO J. 2003;22:6526-6536.
21. Cheng LE, Chan FK, Cado D, Winoto A. Functional redundancy of the Nur77 and Nor-1 orphan steroid receptors in T-cell apoptosis. EMBO J. 1997;16:1865-1875.
22. Li H, Kolluri SK, Gu J, et al. Cytochrome c release and apoptosis induced by mitochondrial targeting of nuclear orphan receptor TR3. Science. 2000;289:1159-1164.
23. Moll UM, Marchenko N, Zhang XK. P53 and Nur77/TR3-transcription factors that directly target mitochondria for cell death induction. Oncogene. 2006;25:4725-4743.
24. Lin B, Kolluri SK, Lin F, et al. Conversion of Bcl-2 from protector to killer by interaction with nuclear receptor Nur77/TR3. Cell. 2004;116:527-540.
25. Thompson J, Winoto A. During negative selection, Nur77 family proteins translocate to mitochondria where they associate with Bcl-2 and expose its proapoptotic BH3 domain. J Exp Med. 2008;205:1029-1036.
26. Zhou T, Cheng J, Yang P, et al. Inhibition of Nur77/Nurr1 leads to inefficient clonal deletion of self-reactive T cells. J Exp Med. 1996;183:1879-1892.
27. Calnan BJ, Szychowski S, Chan FK, Cado D, Winoto A. A role for the orphan steroid receptor Nur77 in apoptosis accompanying antigen-induced negative selection. Immunity. 1995;3:273-282.
28. Weih F, Ryseck RP, Chen L, Bravo R. Apoptosis of nur77/N10-transgenic thymocytes involves the Fas/Fas ligand pathway. Proc Natl Acad Sci U S A. 1996;93:5533-5538.
29. Mullican SE, Zhang S, Konopleva M, et al. Abrogation of nuclear receptors Nr4a3 and Nr4a1 leads to development of acute myeloid leukemia. Nat Med. 2007;13:730-735.
30. Oltersdorf T, Elmore SW, Shoemaker AR, et al. An inhibitor of Bcl-2 family proteins induces regression of solid tumours. Nature. 2005;435:677-681.
31. Konopleva M, Contractor R, Tsao T, et al. Mechanisms of apoptosis sensitivity and resistance to the BH3 mimetic ABT-737 in acute myeloid leukemia. Cancer Cell. 2006;10:375-388.
32. Guo F, Sigua C, Tao J, et al. Cotreatment with histone deacetylase inhibitor LAQ824 enhances Apo-2L/tumor necrosis factor-related apoptosis inducing ligand-induced death inducing signaling complex activity and apoptosis of human acute leukemia cells. Cancer Res. 2004;64:2580-2589.
33. Fiskus W, Pranpat M, Bali P, et al. Combined effects of novel tyrosine kinase inhibitor AMN107 and histone deacetylase inhibitor LBH589 against Bcr-Abl expressing human leukemia cells. Blood. 2006;108:645-652.
34. Edwards A, Li J, Atadja P, Bhalla K, Haura E. Effect of the histone deacetylase inhibitor LBH589 against epidermal growth factor receptor-dependent lung cancer cells. Mol Cancer Ther. 2007;6:2515-2524.
35. George P, Bali P, Annavarapu S, et al. Combination of histone deacetylase inhibitor LBH589 and the hsp90 inhibitor 17-AAG is highly active against human CML-BC cells and AML cells with activating mutation of FLT-3. Blood. 2005;105:1768-1776.
36. Yang Y, Rao R, Shen J, et al. Role of acetylation and extracellular location of heat shock protein 90 alpha in tumor cell invasion. Cancer Res. 2008;68:4833-4842.
37. Ibrado AM, Huang Y, Fang G, Bhalla K. Bcl-xL overexpression inhibits taxol-induced Yama protease activity and apoptosis. Cell Growth Differ. 1996;7:1087-1094.
38. Chou TC, Talalay P. Quantitative analysis of dose-effect relationships: the combined effects of multiple drugs or enzyme inhibitors. Adv Enzyme Regul. 1984;22:7-55.
39. Zhang C, Richon V, Ni X, et al. Selective induction of apoptosis by histone deacetylase inhibitor SAHA in cutaneous T-cell lymphoma cells: relevance to mechanism of therapeutic action. J Invest Dermatol. 2005;125:1045-1052.
40. Fantin VR, Loboda A, Paweletz CP, et al. Constitutive activation of signal transducers and activators of transcription predicts vorinostat resistance in cutaneous T-cell lymphoma. Cancer Res. 2008;68:3785-3794.
41. Khan N, Jeffers M, Kumar S, et al. Determination of the class and isoform selectivity of small-molecule histone deacetylase inhibitors. Biochem J. 2008;409:581-589.
42. Scott FL, Fuchs GJ, Boyd SE, et al. Caspase 8 cleaves histone deacetylase 7 and abolishes its transcription repressor function. J Biol Chem. 2008;283:19499-19510.
43. Fiskus W, Pranpat M, Balasis M, et al. Histone deacetylase inhibitors deplete enhancer of zeste 2 and associated polycomb repressive complex 2 proteins in human acute leukemia cells. Mol Cancer Ther. 2006;5:3096-3104.
44. Fiskus W, Herger B, Rao R, Atadja P, Bhalla K. Pan-HDAC inhibitor LBH589 depletes EZH2 and DNMT1 by inhibiting chaperone association of hsp90 with EZH2 and DNMT1 [abstract]. Proc Am Assoc Can Res. 2007;Abstract 2476.
45. Zhou Q, Agoston AT, Atadja P, Nelson WG, Davidson NE. Inhibition of histone deacetylases promotes ubiquitin-dependent proteasomal degradation of DNA methyltransferase 1 in human breast cancer cells. Mol Cancer Res. 2008;6:873-883.
46. Han YH, Cao X, Lin B, et al. Regulation of Nur77 nuclear export by c-Jun N-terminal kinase and Akt. Oncogene. 2006;25:2974-2986.
47. Wilson AJ, Arango D, Mariadason JM, Heerdt BG, Augenlicht LH. TR3/Nur77 in colon cancer cell apoptosis. Cancer Res. 2003;63:5401-5407.
48. Rapak A, Stasik I, Ziolo E, Strzadala L. Apoptosis of lymphoma cells is abolished due to blockade of cytochrome c release despite Nur77 mitochondrial targeting. Apoptosis. 2007;12:1873-1878.
49. Wright CW, Duckett CS. Reawakening the cellular death program in neoplasia through the therapeutic blockade of IAP function. J Clin Invest. 2005;115:2673-2678.
50. Yu H, Jove R. The STATs of cancer- new molecular targets come of age. Nat Rev Cancer. 2004;4:97-105.
51. Vogler M, Dinsdale D, Dyer MJ, Cohen GM. Bcl-2 inhibitors: small molecules with a big impact on cancer therapy. Cell Death Differ. 2009;16:360-367.